RAPID COMMUNICATIONS

PHYSICAL REVIEW B VOLUME 51, NUMBER 22 1 JUNE 1995-II

Observation of a possible oxygen isotope effect on the effective mass of carriers in $YBa_2Cu_3O_{6.94}$

Guo-meng Zhao* and Donald E. Morris
Morris Research Inc., 1918 University Avenue, Berkeley, California 94704
(Received 26 January 1995; revised manuscript received 14 March 1995)

We have investigated oxygen-isotope effects on the effective mass of carriers m^* and carrier concentration n_s in fine-grained $YBa_2Cu_3O_y$ ($y \approx 6.94$) using measurements of onset magnetizations in Meissner and mixed states. We find a large negative oxygen-isotope effect on m^* with an exponent $\alpha_{Om^*} = -d\ \ln(m^*)/d\ \ln M_O = -0.61 \pm 0.09$, and a small oxygen-isotope effect on n_s with an exponent $\alpha_{On} = -d\ \ln(n_s)/d\ \ln M_O = 0 \pm 0.13$. We also observe a small positive oxygen-isotope effect on T_c with an exponent $\alpha_O = -d\ \ln T_c/d\ \ln M_O = 0.028 \pm 0.002$. The large oxygen-isotope effect on m^* can be explained as due to the breakdown of the Migdal approximation and/or strong anharmonicity of phonon modes.

It is now well established that the optimally doped cuprates show a small oxygen-isotope effect while the underdoped cuprates show a large oxygen-isotope effect.[1–9] Franck *et al.*[10] have investigated copper- and oxygen-isotope effects in optimally doped and underdoped $La_{2-x}Sr_xCuO_4$, and found that the copper- and oxygen-isotope exponents have similar magnitudes.

The observed large isotope effect for the underdoped cuprates may point to the phonon-mediated pairing mechanisms for high-T_c superconductivity. Muon-spin-relaxation (μSR) experiments have, however, shown a universal linear relation: $T_c \propto n_s/m^*$ for the undoped cuprates,[11] where n_s is the superfluid density and m^* is the effective mass of carriers. Then the large isotope effect on T_c for the underdoped cuprates can be explained as due to the isotope effects on m^* and/or n_s. The question is whether there also exist isotope effects on m^* and/or n_s in the optimally doped cuprates.

Here we report the deduction of oxygen-isotope effects on the effective mass of carriers m^* and carrier concentration n_s from measurements of onset magnetizations in Meissner and mixed states in fine-grained $YBa_2Cu_3O_y$ ($y \approx 6.94$). We find a large negative oxygen-isotope effect on m^* and a small oxygen-isotope effect on n_s. The large oxygen-isotope effect on m^* can be explained as due to the breakdown of the Migdal approximation.

The samples were prepared from high-purity Y_2O_3 (99.99%), $BaCO_3$ (99.999%), and Cu (99.999%). We first prepared the mixtures of Y_2O_3 and $BaCO_3$ with the required stoichiometric ratio of Y and Ba. The mixtures were, respectively, combined with two stoichiometric amounts of CuO for preparing two samples. The two powder mixtures were placed in separate gold boats and calcined at 920 °C for 15 h in flowing oxygen (70 cc/min). The two samples were then ground for ~15 min, respectively, pelletized and sintered at 920 °C for 15 h in flowing oxygen. To ensure that the samples have small grain size and enough porosity, we reground the two samples, respectively, pelletized and annealed them in flowing oxygen at 800 °C for 10 h, and at 600 °C for 24 h, and cooled to 300 °C for 24 h, and then cooled to room temperature for 12 h. The above procedure has been used by us to investigate the copper-isotope effect.

The two pelletized samples were broken into halves (producing two sample pairs), and the halves were subject to the ^{16}O- and ^{18}O-isotope diffusion, which was conducted in two parallel quartz tubes separated by about 2 cm.[4,7] The diffusion was done for 20 h at 670 °C and oxygen pressure of ~1.0 bar. The cooling time from 670 to 120 °C was 11 h (50 °C/h). The oxygen-isotope enrichment was determined from the weight changes of the ^{16}O and ^{18}O samples. The ^{18}O samples had ~95% ^{18}O and ~5% ^{16}O. The lattice constants of the samples were determined to be $a = 3.821$ Å, $b = 3.884$ Å, and $c = 11.687$ Å, corresponding to the oxygen content of 6.94 ± 0.01.[12]

The susceptibility was measured with a Quantum Design SQUID magnetometer. The field-cooled, measured-on-warming (FCW) susceptibility was measured in a field of ~1.0, 10, or 150 Oe. The temperature measurements were performed with a platinum resistance thermometer (Lakeshore PT-111) placed in direct contact with the sample and driven by a microprocessor-controlled ac bridge in the SQUID. The resolution is 2.5 mK and reproducibility is 10 mK at 77 K after cycling to room temperature. All samples were carefully aligned in the same direction (along the axis parallel to the field) during each measurement. The data were collected upon warming. The field was kept unchanged throughout the whole series of measurements.

In Figs. 1(a) and 1(b), we show the susceptibility near T_c for the ^{16}O and ^{18}O samples of (a) pair I and (b) pair II. The magnetic field for measurements is ~10 Oe. At low temperatures, the susceptibility of the ^{16}O samples is $\sim 1.5 \pm 1.0\%$ larger than that of the ^{18}O samples. There are well-defined linear portions on the transition curves starting just ~0.5 K below the diamagnetic onset temperatures. The negative curvature near T_c (~0.5 K range) is due to $H_{ext} > H_{c1}(T)$, and to the fluctuation and/or inhomogeneity. From Figs. 1(a) and 1(b), we find that the exponent of the oxygen-isotope effect on T_c is $\alpha_O = -d\ \ln T_c/d\ \ln M_O = 0.028 \pm 0.002$, which is similar to that ($\alpha_O = 0.025 \pm 0.002$) for the sample with $y \sim 6.95 \pm 0.03$.[7]

From Figs. 1(a) and 1(b), we also note that the slopes of the linear portions (denoted by P_1) for the ^{18}O samples are $\sim 7 \pm 1$ % smaller than for the ^{16}O samples. Since there are distinct curvatures beyond the linear portions, one has to draw the linear lines objectively. So we first select data points by inspection to get a best linear fit, then increase data

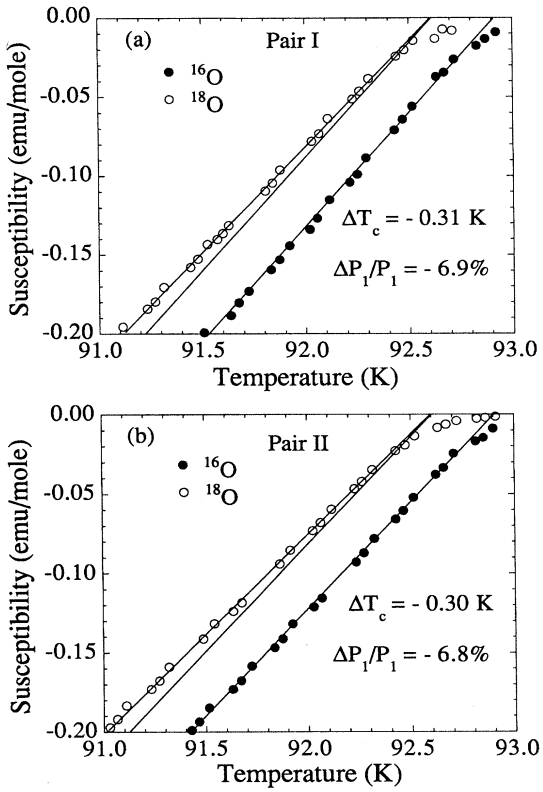

FIG. 1. The FCW susceptibility near T_c for (a) pair I and (b) pair II, measured in a magnetic field of 10 Oe. The oxygen isotope shift is $\Delta T_c = -0.31 \pm 0.02$ K. The slopes of the linear portions on the transition curves (denoted by P_1) are different for the ^{16}O and ^{18}O samples ($\Delta P_1/P_1 = -7 \pm 1$ %). The in-between straight lines in (a) and (b) are parallel to the lines for the ^{16}O samples.

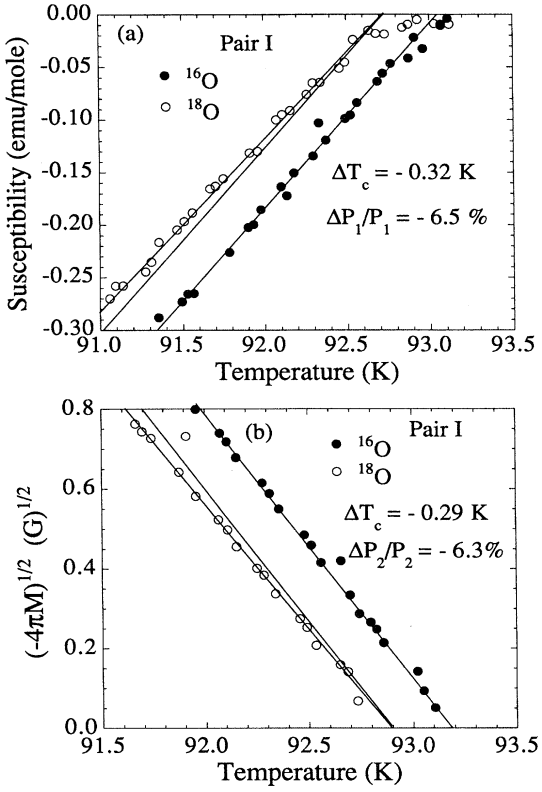

FIG. 2. (a) The FCW susceptibility near T_c for pair I, measured in a field of 1.0 ± 0.1 Oe. The measured oxygen-isotope effects on T_c and P_1 are the same as those shown in Fig. 1(a). (b) The plot of $(-4\pi M)^{1/2}$ vs T for pair I, measured in a field of 150 Oe. The slopes of the linear portions on the transition curves (denoted by P_2) are different for the ^{16}O and ^{18}O samples ($\Delta P_2/P_2 = -7 \pm 1$ %).

points one by one until the fit gets worse. We also ensure the similar temperature intervals of the linear portions for the ^{16}O and ^{18}O samples to minimize the uncertainty of the relative difference in the slopes. Since the linear portions have ~ 20 high-quality data points which can be obtained through our thermometer probe, the relative differences in the slopes of the linear portions have a small uncertainty. A similar result was also observed in another optimally doped system $La_{1.85}Sr_{0.15}CuO_4$.[5]

In Fig. 2(a), we show the susceptibility near T_c for the ^{16}O and ^{18}O samples of pair I, which was measured in a field of 1.0 ± 0.1 Oe. The negative curvature near T_c now has a range of ~ 0.2 K, an upper limit of the fluctuation and/or inhomogeneity range. Comparing Figs. 1(a) and 2(a), one can see that the oxygen isotope effects on P_1 (the slope of the linear portion) and T_c are independent of the magnetic field although the magnitude of P_1 does depend on the magnetic field slightly. This implies that the observed isotope effect on P_1 is not likely caused by the differences in flux pinning of the ^{16}O and ^{18}O samples. The small field dependence of P_1 indicates a possible presence of weak links between the grains of some clusters which may consist of several grains. In the case of low magnetic fields, it is possible to show that the susceptibility depends on the effective size of the cluster $R_{\text{eff}}(H)$, instead of the grain size R.[13]

The magnetization data taken by cooling the sample in a magnetic field of 150 Oe are shown in Fig. 2(b) for sample pair I. The data are plotted as $(-4\pi M)^{1/2}$ vs T, since M is found to vary approximately as $(1-T/T_c)^2$ near T_c, as shown by Finnemore *et al.*[14] Such a temperature dependence is to be expected for a material composed of phase-decoupled (or only very weakly Josephson-coupled) superconducting grains with linear dimensions comparable to the penetration depth.[14] There are indeed well-defined linear portions near T_c. The slope of the linear portion (denoted by P_2) for the ^{18}O sample is also smaller than for the ^{16}O sample. Comparing Fig. 2(b) with Figs. 1(a) and 2(a), we find that the oxygen-isotope effects on P_1 and P_2 are the same within the uncertainty, and that the temperature ranges of the linear portions are similar in both cases. However, the physics shown in Fig. 2(a) is different from that shown in Fig. 2(b). The former shows the susceptibility in the Meissner state while the latter shows the magnetization in the mixed state where $H_{\text{ext}} > H_{c1}(T)$.

In Fig. 3(a), we show the susceptibility near T_c for the two ^{16}O samples measured in a field of ~ 10 Oe. The two samples were treated in the same conditions except that they were ground and pelletized separately. So they have the same T_c but may have slightly different grain size and thus the

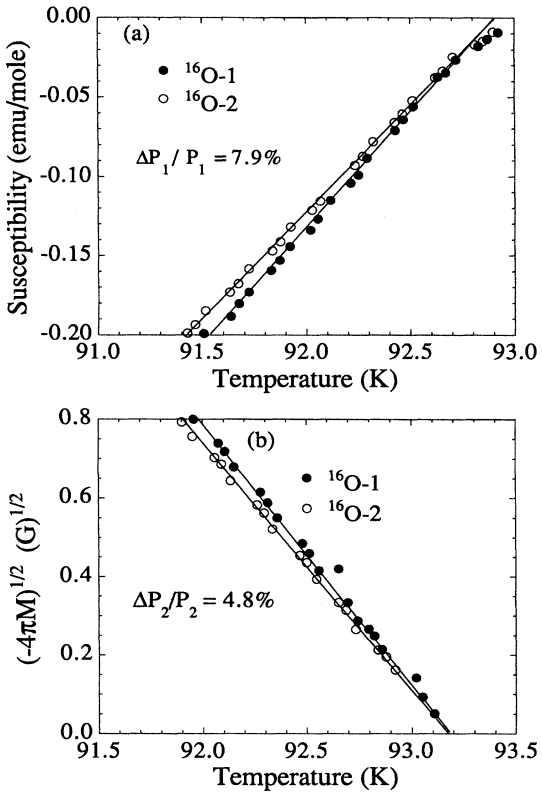

FIG. 3. (a) The FCW susceptibility near T_c for two ^{16}O samples, measured in a field of 10 Oe. (b) The plot of $(-4\pi M)^{1/2}$ vs T for two ^{16}O samples, measured in a field of 150 Oe. The two samples were treated in the same conditions except that they were ground and pelletized separately, so they may have slightly different grain sizes, and thus different P_1 and P_2. The relation $\Delta P_1/P_1 \approx 2\Delta P_2/P_2$, deduced from the figures is consistent with Eqs. (1) and (4) (see text).

slope P_1. In Fig. 3(b), we plot $(-4\pi M)^{1/2}$ vs T for the two ^{16}O samples measured in a field of 150 Oe. Comparing Figs. 3(a) and 3(b), we find that $\Delta P_1/P_1 \approx 2\Delta P_2/P_2$. This can be explained as either due to the difference in demagnetization factors of the two samples, or due to the slight difference in grain sizes of the two samples as seen from Eqs. (1) and (4) below.

A possible route for understanding the above isotope data is that the penetration depth may depend on the oxygen mass. It is known that the Meissner fraction $f(T)$ for fine-grained and decoupled samples is reduced due to the penetration depth which is comparable with the radii of grains. Near T_c, the penetration depth will be large, so that above a temperature (called T^*), there exists a condition that $\lambda_c(T) > \lambda_{ab}(T) > r$, where r is the radius of a grain, $\lambda_{ab}(T)$ is the in-plane penetration depth (along CuO plane), and $\lambda_c(T)$ is the out-of-plane penetration depth. In this case, the Meissner fraction is given by $f(T) \sim R^2/15\lambda(T)^2$ (Ref. 13) [where R is the average radius of grains and $\lambda(T)$ is the effective penetration depth]. Using $\lambda_c(T) \sim 5\lambda_{ab}(T)$,[15] and $\lambda(T)^3 = [\lambda_{ab}(T)]^2\lambda_c(T)$,[16] we have $f(T) \sim R^2/44[\lambda_{ab}(T)]^2$. For weakly coupled grains, the above relation is still valid in the low field range if one uses $R_{\rm eff}(H)$, instead of R.[13] From the above relation and measured Meissner susceptibility (with a correction of a demagnetization factor of $\frac{1}{3}$), we estimate $T_c - T^* \sim 1.5$ K at which $R = \lambda_{ab}(T^*)$ and $f(T^*) = 1/44$. So the above relations hold for $T_c - T < 1.5$ K. Near T_c, there is a relation: $\lambda(T)^2 \propto \lambda(0)^2/(1 - T/T_c)$, then the slope of the linear portion (denoted as P_1) is

$$P_1 = df(T)/dT \propto R^2/T_c\lambda(0)^2 \propto R^2 n_s/T_c m^*. \quad (1)$$

Since there is a small oxygen-isotope effect on T_c for optimally doped cuprates, the large oxygen-isotope effect on P_1 indicates that there is a large oxygen-isotope effect on n_s and/or m^* (the average grain radii of the ^{16}O and ^{18}O samples must be the same since they are from the same pellet and have the same susceptibility before isotope exchange). From Eq. (1), we obtain

$$\Delta P_1/P_1 = \Delta n_s/n_s - \Delta T_c/T_c - \Delta m^*/m^*, \quad (2)$$

where Δ means the isotope-induced change.

When the applied magnetic field $H_{\rm ext} > H_{c1}(T)$, Finnemore *et al.*[14] have shown that

$$(-4\pi M)^{1/2} \propto R[T_c(H) - T] \times [|dH_{c2}/dT|/(2\kappa^2 - 1)T_c]^{1/2}/\lambda(0). \quad (3)$$

Using the clean-limit Werthamer-Helfand-Hohenberg formula, $[|dH_{c2}/dT|/T_c]^{1/2} \propto \gamma \propto n_s^{1/3}m^*$, and $1 \ll \kappa = \lambda(0)/\xi(0) \propto \lambda(0)T_c m^*/n_s^{1/3}$, we have $(-4\pi M)^{1/2} \propto R[T_c(H) - T]n_s^{2/3}/\lambda(0)^2 T_c$, and the slope P_2:

$$P_2 = d(-4\pi M)^{1/2}/dT \propto Rn_s^{2/3}/\lambda(0)^2 T_c \propto Rn_s^{5/3}/T_c m^*. \quad (4)$$

For a two-dimensional system, the $n_s^{5/3}$ in Eq. (4) will be replaced by $n_s^{3/2}$. Comparing Eqs. (1) and (4), one can see that the slopes P_1 and P_2 have different power dependences on n_s but the same power dependence on m^* and T_c. So the isotope effect on P_2 will nearly double the isotope effect on P_1 if there only exists an isotope effect on n_s, in contradiction with the observed results. From Eq. (4), we have

$$\Delta P_2/P_2 = \tfrac{5}{3}\Delta n_s/n_s - \Delta T_c/T_c - \Delta m^*/m^*. \quad (5)$$

Substituting $\Delta P_1/P_1 \approx \Delta P_2/P_2 = (7 \pm 1)\%$, $\Delta T_c/T_c = (-0.34 \pm 0.02)\%$ into Eqs. (2) and (5), we get $\Delta m^*/m^* = (7.3 \pm 1.0)\%$, and $\Delta n_s/n_s = (0 \pm 1.5)\%$, corresponding to $\alpha_{Om^*} = -d\ \ln(m^*)/d\ \ln M_O = -0.61 \pm 0.09$, and $\alpha_{On} = -d\ \ln(n_s)/d\ \ln M_O = 0 \pm 0.13$.

From the oxygen-isotope effect on n_s, we can estimate a difference in the oxygen contents of the ^{16}O and ^{18}O samples due to slightly different diffusion rates for the two isotope samples. Since the total carrier concentration in $YBa_2Cu_3O_7$ is $n_s \sim 5 \times 10^{21}/\text{cm}^3$,[17] then $\Delta n_s = (0 \pm 1.5\%)n_s = (0 \pm 7.5) \times 10^{19}/\text{cm}^3$ which corresponds to 0 ± 0.007 oxygen per cell if each oxygen contributes two holes to the total carrier system on chains and planes. Then the oxygen contents of the ^{16}O and ^{18}O samples are the same within ± 0.007 oxygen per cell. So the slightly different diffusion rates for the ^{16}O and ^{18}O samples lead to a small difference in oxygen contents, in agreement with Ref. 18 which has

shown that the ^{16}O and ^{18}O samples of La_2CuO_{4+y} have the same oxygen content within ± 0.0001 oxygen per cell.

The observed isotope effects are not consistent with the microscopic model for the isotope effect as proposed by Kresin and Wolf.[19] In their model, they assume a large asymmetry in the double-well potential for the apical oxygen, which has not been justified experimentally. Furthermore, we have done site-selective oxygen isotope exchange at 320 °C for 100 h and obtained the site-selective ^{18}O sample with ~ 85–$95\ \%$ ^{18}O in CuO planes, $\sim 100\%$ ^{16}O in apical and chain positions. For these site-selective samples, we have also found that the slope P_1 for the ^{18}O sample is $\sim 4\%$ smaller than for the ^{16}O sample. This result rules out the explanation by Kresin and Wolf, since the site-selective samples have the same oxygen isotope in the apical and chain positions. On the other hand, the internal charge transfer, if it depends on the oxygen mass,[19] will not change the total n_s since the holes in the chains are also supercarriers.[20]

In a general BCS-like treatment, the total coupling constant λ_t (from phonon and any other bosonic excitations) is given by $\lambda_t = N(E_f)V_t$, where V_t is the total pairing potential and $N(E_F)$ is the average density of states. In clean superconductors, the renormalization factor $(1+\lambda_t)$ enters into the penetration depth, coherence length, and Sommerfield constant as shown by Carbotte.[21] The effective mass of carriers m^* is then proportional to $N(E_F)(1+\lambda_t) = N(E_F)[1+N(E_F)V_t]$. From the above relation and observed oxygen-isotope effect on m^*, one can see that the $N(E_F)$ and/or V_t will depend on the oxygen mass, in contrast to conventional superconductors where both $N(E_F)$ and V_t are independent of ion mass. So our results cannot be explained by conventional models.

There are several possible theoretical explanations for the oxygen-mass dependence of the $N(E_F)$. Pickett *et al.*[22] have shown that the strong anharmonicity of phonon modes will make $N(E_F)$ depend on the ion mass due to structure fluctuation. However, there is no evidence that the strong anharmonicity is present in $YBa_2Cu_3O_y$.[22] Alternatively, the ion-mass dependence of $N(E_F)$ could be due to the breakdown of the Migdal adiabatic approximation. Engelesberge and Schrieffer[23] have shown that the Migdal approximation does not hold if there is a reasonably strong interaction between electrons and long-wavelength optical phonons. For short-wavelength optical phonons, however, the Migdal approximation still holds.[23] The breakdown of the Migdal approximation will lead to the formation of polarons.[24] The interaction of the electrons with the long-wavelength optical phonons (or the local phonons as in the Holstein model) narrows the electronic bandwidth and enhances the density of states by a factor $A(\omega)\exp(B/\omega)$ which is ion mass dependent.[24] Nevertheless, these long-wavelength optical phonons (or the local phonons) have little contribution to the k-space pairing potential[25] since the phase space for the processes of small-momentum transfer is small. It is rather the large-momentum transfers which are important in bringing about superconductivity.[25]

Since the long-wavelength optical phonons (or local phonons) play different roles from the short-wavelength phonons, one will expect that the strong-coupling Eliashberg theory may still hold if one uses the enhanced $N(E_F)$ (due to the interaction between the electrons and long-wavelength optical phonons), instead of the bare state density calculated from the rigid lattice. Within this model, we can quantatively explain the large negative isotope effect on m^* and the small positive isotope effect on T_c in $YBa_2Cu_3O_7$. The details will be given elsewhere.

In summary, we have deduced oxygen-isotope effects on the effective mass of carriers m^* and carrier concentration n_s in $YBa_2Cu_3O_y$ ($y \approx 6.94$). We show a possible large oxygen-isotope effect on m^* with an exponent $\alpha_{Om^*} = -d\ \ln(m^*)/d\ \ln M_O = -0.61 \pm 0.09$, and a small oxygen-isotope effect on n_s. The large oxygen-isotope effect on m^* can be explained as due to the breakdown of the Migdal approximation.

*At the Department of Physics, University of Texas at Austin after August 1995.

[1] B. Batlogg *et al.*, Phys. Rev. Lett. **58**, 2333 (1987).
[2] L. C. Bourne *et al.*, Phys. Rev. Lett. **58**, 2337 (1987).
[3] D. E. Morris *et al.*, Phys. Rev. B **37**, 5936 (1988).
[4] J. H. Nickel, D. E. Morris, and J. W. Ager, III, Phys. Rev. Lett. **70**, 81 (1993).
[5] M. K. Crawford *et al.*, Phys. Rev. B **41**, 282 (1990).
[6] M. K. Crawford *et al.*, Science **250**, 1390 (1990).
[7] H. J. Bornemann and D. E. Morris, Phys. Rev. B **44**, 5322 (1991).
[8] J. P. Franck *et al.*, Phys. Rev. B **44**, 5318 (1991).
[9] E. L. Benitez *et al.*, Phys. Rev. B **38**, 5025 (1988).
[10] J. P. Franck *et al.*, Phys. Rev. Lett. **71**, 283 (1993).
[11] Y. J. Uemura *et al.*, Phys. Rev. Lett. **62**, 2317 (1989).
[12] J. D. Jorgensen *et al.*, Phys. Rev. B **41**, 1863 (1990).
[13] A. M. Neminsky *et al.*, Phys. Rev. Lett. **72**, 3092 (1994).
[14] D. K. Finnemore *et al.*, Phys. Rev. B **35**, 5319 (1987).
[15] B. Pumpin *et al.*, Physica C **162-164**, 151 (1989).
[16] T. Nagano *et al.*, Phys. Rev. B **48**, 9689 (1993).
[17] X. X. Xi *et al.*, Phys. Rev. Lett. **68**, 1240 (1990).
[18] Guo-meng Zhao, K. K. Singh, and Donald E. Morris, Phys. Rev. B **50**, 4112 (1994).
[19] V. Z. Kresin and S. A. Wolf, Phys. Rev. B **49**, 2652 (1994).
[20] J. L. Tallon *et al.*, Phys. Rev. Lett. **74**, 1008 (1995).
[21] J. P. Carbotte, Rev. Mod. Phys. **62**, 1027 (1990).
[22] W. E. Pickett, R. E. Cohen, and H. Krakauer, Phys. Rev. Lett. **67**, 228 (1991).
[23] S. Engelesberge and J. R. Schrieffer, Phys. Rev. **131**, 993 (1963).
[24] A. S. Alexandrov and N. F. Mott, Int. J. Mod. Phys. B **8**, 2075 (1994).
[25] J. R. Schrieffer, *Theory of Superconductivity*, edited by D. Pines (Addison-Wesley, New York, 1988), p. 99.